

# REPORT DOCUMENTATION PAGE

Form Approved  
OMB NO. 0704-0188

Public Reporting burden for this collection of information is estimated to average 1 hour per response, including the time for reviewing instructions, searching existing data sources, gathering and maintaining the data needed, and completing and reviewing the collection of information. Send comment regarding this burden estimates or any other aspect of this collection of information, including suggestions for reducing this burden, to Washington Headquarters Services, Directorate for information Operations and Reports, 1215 Jefferson Davis Highway, Suite 1204, Arlington, VA 22202-4302, and to the Office of Management and Budget, Paperwork Reduction Project (0704-0188,) Washington, DC 20503.

1. AGENCY USE ONLY ( Leave Blank)		2. REPORT DATE	3. REPORT TYPE AND DATES COVERED Peer Reviewed Reprint	
4. TITLE AND SUBTITLE Shock Tube Measurements of Iso-Octane Ignition Times and OH Concentration Time Histories			5. FUNDING NUMBERS DAAD19-01-1-0597	
6. AUTHOR(S) D. F. Davidson M.A. Oehlschlaeger, J. T. Herbon, and R. K Hanson				
7. PERFORMING ORGANIZATION NAME(S) AND ADDRESS(ES) Stanford University, Mechanical Engineering Department Building 520, Duena Street Stanford CA, 94305-3032			8. PERFORMING ORGANIZATION REPORT NUMBER	
9. SPONSORING / MONITORING AGENCY NAME(S) AND ADDRESS(ES) U. S. Army Research Office P.O. Box 12211 Research Triangle Park, NC 27709-2211			10. SPONSORING / MONITORING AGENCY REPORT NUMBER  41100.1-EG	
11. SUPPLEMENTARY NOTES The views, opinions and/or findings contained in this report are those of the author(s) and should not be construed as an official Department of the Army position, policy or decision, unless so designated by other documentation.				
12 a. DISTRIBUTION / AVAILABILITY STATEMENT  Approved for public release; distribution unlimited.			12 b. DISTRIBUTION CODE	
13. ABSTRACT (Maximum 200 words)  Ignition times and OH radical concentration time histories were measured behind reflected shock waves in iso-octane/O <sub>2</sub> /Ar mixtures. Initial reflected shock conditions were in the ranges 1177 to 2009 K and 1.18 to 8.17 atm, with fuel concentrations of 100 ppm to 1% and equivalence ratios from 0.25 to 2. Ignition times were measured using endwall emission of CH and sidewall pressure. OH concentrations were measured using narrow-linewidth ring-dye laser absorption of the R <sub>1</sub> (5) line of the OH A-X (0,0) band at 306.5 nm. The ignition time data and OH concentration time history measurements were compared to model predictions of four current iso-octane oxidation mechanisms, and the implications of these comparisons are discussed. To our knowledge, these data provide the first extensive measurements of low fuel-concentration ignition times and OH concentration time histories for iso-octane auto-ignition, and hence provide a critical contribution to the database needed for validation of a detailed mechanism for this primary reference fuel.				
14. SUBJECT TERMS Ignition Times, Shock Tubes, iso-octane, OH laser absorption			15. NUMBER OF PAGES 7	
			16. PRICE CODE	
17. SECURITY CLASSIFICATION OR REPORT <b>UNCLASSIFIED</b>	18. SECURITY CLASSIFICATION ON THIS PAGE <b>UNCLASSIFIED</b>	19. SECURITY CLASSIFICATION OF ABSTRACT <b>UNCLASSIFIED</b>	20. LIMITATION OF ABSTRACT  <b>UL</b>	

NSN 7540-01-280-5500

Standard Form 298 (Rev.2-89)  
Prescribed by ANSI Std. Z39-18  
298-102

## SHOCK TUBE MEASUREMENTS OF ISO-OCTANE IGNITION TIMES AND OH CONCENTRATION TIME HISTORIES

D. F. DAVIDSON, M. A. OEHLSCHLAEGER, J. T. HERBON AND R. K. HANSON

*High Temperature Gasdynamics Laboratory  
Mechanical Engineering Department  
Stanford University, Stanford, CA 94305, USA*

Ignition times and OH radical concentration time histories were measured behind reflected shockwaves in iso-octane/O<sub>2</sub>/Ar mixtures. Initial reflected shock conditions were in the ranges 1177 to 2009 K and 1.18 to 8.17 atm, with fuel concentrations of 100 ppm to 1% and equivalence ratios from 0.25 to 2. Ignition times were measured using endwall emission of CH and sidewall pressure. OH concentrations were measured using narrow-linewidth ring-dye laser absorption of the R<sub>1</sub>(5) line of the OH A-X (0,0) band at 306.5 nm. The ignition time data and OH concentration time-history measurements were compared with model predictions of four current iso-octane oxidation mechanisms, and the implications of these comparisons are discussed. To our knowledge, these data provide the first extensive measurements of low-fuel-concentration ignition times and OH concentration time histories for iso-octane autoignition, and hence provide a critical contribution to the database needed for validation of a detailed mechanism for this primary reference fuel.

### Introduction

Iso-octane is an important component of practical fuels. It is also used as the high-octane-number primary reference fuel in the development of surrogate fuel mixtures for gasoline engine chemistry modeling. Increasing the fraction of iso-octane relative to *n*-heptane in primary reference fuel mixtures is well known to reduce knock in engines. This effect is attributed to the strong radical scavenging, primarily of OH, of the iso-octane oxidation pathways in competition with the reactive *n*-heptane oxidation pathways [1]. Few, if any, studies exist that provide direct information on the OH concentration time histories that occur during iso-octane autoignition.

The chemistry of iso-octane oxidation is also evident in shock tube ignition time studies where the branched-chain iso-octane has been shown to have longer ignition times than the straight-chain *n*-octane [2]. However, the use of iso-octane ignition times as model validation targets is complicated by the fact that there does not appear to be a consensus among the various shock tube studies [2–6] and that few studies have correlated their findings with those of other workers to allow quantitative comparison.

The chemical kinetic validation of iso-octane reaction mechanisms currently relies on a wide variety of target data including ignition-delay times, flame speeds, and species concentration time histories in various combustors and flow reactors. Currently, only stable species such as O<sub>2</sub>, CO, CO<sub>2</sub>, and H<sub>2</sub>O, and long-lived hydrocarbon intermediate species, mostly measured using gas chromatography, are

used as targets. Very limited information is available on the important transient radical pool (O, H, OH, HO<sub>2</sub>, and CH<sub>3</sub>) responsible for H-abstraction reactions or branching processes. This is not an oversight on the part of these mechanism development studies (see, for example, Refs. [7–10]); these data simply do not exist for larger fuel molecules, yet they are urgently needed if the predictive ability of these mechanisms is to be tied to the actual kinetics of the radical pool population.

Many of the current iso-octane reaction mechanisms are derived from the large reference fuel mechanism developed at Lawrence Livermore National Laboratory (LLNL) by Westbrook and co-workers. In this paper, we will examine three of these mechanisms: Curran et al. [7], Pitsch et al. [8], and Davis and Law [9], as well as a mechanism developed separately in Europe by Ranzi et al. [10].

The very large Curran et al. iso-octane mechanism has approximately 1000 species and 4000 reactions and represents a relatively recent version of the full LLNL mechanism. The Davis and Law mechanism (69 species and 406 reactions) was formed by adding iso-octane-specific reactions from Curran et al. to the Held et al. [11] reduced mechanism for *n*-heptane. In this mechanism, the major olefin products of iso-octane decomposition are C<sub>3</sub>H<sub>6</sub> and *i*-C<sub>4</sub>H<sub>8</sub>, through which all major reaction products pass. The Pitsch et al. mechanism includes 47 species and 134 reactions and is an extension of their reduced mechanism and was developed for use in full engine calculations [8]. The Ranzi et al. mechanism uses 145 species and 2500 reactions and was developed using

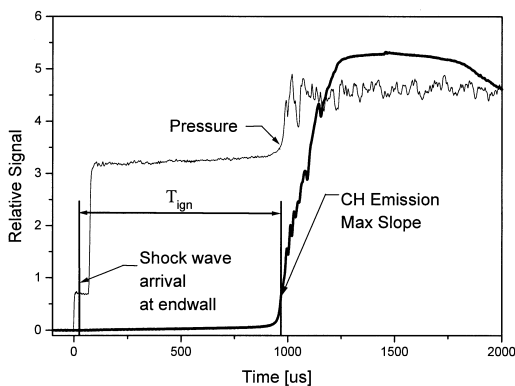


FIG. 1. Iso-octane ignition: CH emission profile and PZT pressure trace. Initial shock conditions: 0.25% iso-octane, 6.25% O<sub>2</sub> 1269 K, 8.07 atm. Ignition time is 952  $\mu$ s.

reaction classes and a lumped kinetic scheme and includes submechanisms from their earlier work on *n*-heptane. (See Ref. [10] for further details.) The need to form smaller mechanisms by reducing the number of species and reactions, and therefore making these mechanisms more amenable to use in full engine calculations, must be tempered by the need to accurately capture the important engineering characteristics of the fuel. The ability of these mechanisms to do this in the case of high-temperature ignition times and OH concentration time histories will be demonstrated in this study.

In the hydrocarbon fuel research program at Stanford, we are attempting to improve and extend the database of kinetic targets used in the testing and validation of detailed (and reduced) mechanisms. Recent work has included the measurement of ignition times and OH and C<sub>2</sub>H<sub>4</sub> concentration time histories for four *n*-alkanes: propane, *n*-butane, *n*-heptane, and *n*-decane [12,13]. In these studies, significant differences were noted between the measured OH and C<sub>2</sub>H<sub>4</sub> concentration time profiles and those predicted by several current mechanisms. The value of this type of data was evident, as previously, there was no other direct method to test the ability of these mechanisms to predict radical pool populations.

In this paper, we present new data for ignition times and OH concentration time histories in the iso-octane oxidation system. These data are correlated and compared with modeling results using the four kinetic mechanisms noted above. The kinetic implications of these comparisons are also discussed.

### Experimental Method

All ignition times were measured in the reflected shock region of either a 14.0 or 15.24 cm diameter, high-purity, helium-driven, shock tube. The shock

velocity at the endwall was calculated from four incident shock wave velocity measurements obtained over the last 1.5 m of the shock tube. Reflected shock conditions were determined from the standard one-dimensional shock relations and the Sandia thermodynamic database, which was amended to include the thermodynamic data for iso-octane from Burcat and McBride [14]. Uncertainty in the initial reflected shock temperature is estimated at  $\pm 10$  K, resulting in about a 10% uncertainty in the measured ignition time. Research grade argon and oxygen and 99.7+ % HPLC grade iso-octane (Aldrich) were used in all mixtures. Initial reflected shock conditions of these measurements were in the ranges of 1177–2009 K and 1.18–8.17 atm, with fuel concentrations of 100 ppm to 1% and equivalence ratios,  $\Phi$ , from 0.25 to 2.

Ignition time measurements are subject to a high degree of experimental scatter and uncertainty if the composition of the test mixture is not accurately measured, or if these measurements are made at a significant distance from the endwall. (See Horning et al. [15] for a discussion of these effects and efforts made to minimize such error in our facility.) Ignition times in this study were measured using CH emission viewed through the shock tube endwall. CH emission was collected using a 431 nm filter with a spectral width of 10 nm and a fast (1.6  $\mu$ s risetime) silicon photodetector. The endwall ignition time is defined as the time interval between the shock arrival at the endwall, which is determined from the incident shock velocity, and the maximum rate of increase in the CH emission signal (see Fig. 1).

OH absorption data were acquired across the diameter of the shock tube 2 cm from the endwall using narrow-linewidth ring-dye laser absorption. The absolute OH concentrations were measured using a standard two-beam laser absorption technique developed in our laboratory (see Herbon et al. [16] for a complete description) using the well-characterized R<sub>1</sub>(5) line of the OH A<sup>2</sup> $\Sigma^+$  – X<sup>2</sup> $\Pi$ (0,0) band. The largest uncertainties in the OH concentration stem from the OH oscillator strength ( $\pm 2\%$ ) and the collisional broadening parameter, yielding total uncertainties in  $X_{OH}$  in the range of 2%–5% for the conditions of the current work. Off-line measurements revealed evidence of a weak, but broadly absorbing species. This absorption, likely from conjugated olefins, is similar to that seen in our earlier study of OH absorption in JP-10 ignition [17], but not seen in our study of *n*-heptane and other *n*-alkanes [12]. The interference absorption was subtracted from the on-line absorption data to determine the corrected OH concentration time histories. An example OH data trace and the results of the subtraction process are shown in Fig. 2. The large signal-to-noise ratio and high sensitivity of this diagnostic permit measurement of parts per million levels of OH at microsecond time resolution.

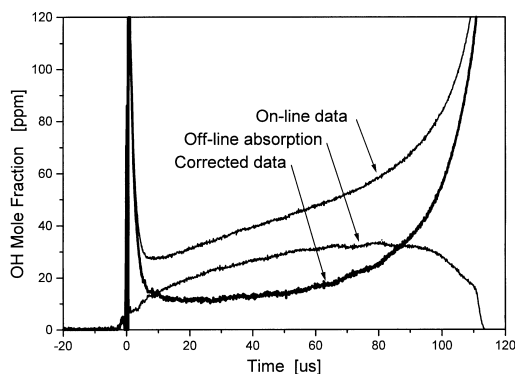


FIG. 2. OH absorption: on-line, off-line, and corrected profile. Initial shock conditions: 1.0% iso-octane, 6.25% O<sub>2</sub>, 1656 K, 1.34 atm. Reflected shock arrival,  $t = 0$ ; ignition,  $t = 116 \mu\text{s}$ .

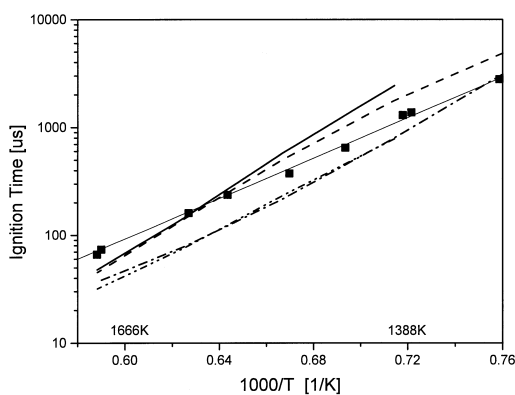


FIG. 3. Variation of ignition time with temperature:  $\Phi = 1.0$ . Initial shock conditions: 0.5% iso-octane, 6.25% O<sub>2</sub> 1.3 atm. Filled squares, current study; thin solid line, fit to data with  $E_A = 43.9 \text{ kcal/mol}$ ; solid line, Davis and Law [9]; dashed line, Ranzi et al. [10]; dot-dashed line, Pitsch et al. [8]; dot-dot-dashed line, Curran et al. [7].

## Experimental Results and Discussion

### Ignition Time Data

The ignition time data are presented as follows. First, the effects of temperature and fuel concentration on ignition time are presented, for a fixed equivalence ratio of 1 (Figs. 3 and 4). Second, the effects of equivalence ratio on ignition time are shown (Fig. 5). Third, a correlation is presented for the ignition time data set (Fig. 6).

The current ignition time data, in general, have very small scatter, as a result of accurate mixture concentration and shock-speed determinations, and the use of endwall CH emission as a direct indicator of ignition time. In the correlation presented below,

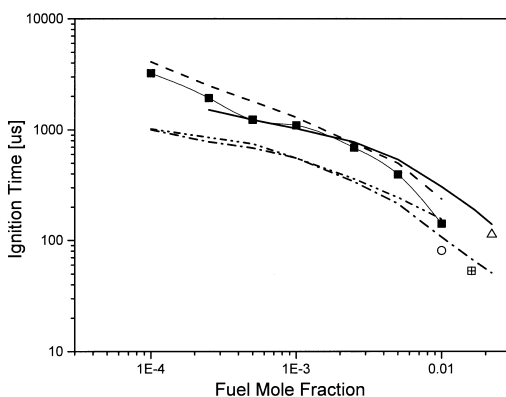


FIG. 4. Variation of ignition time with fuel concentration. Initial shock conditions:  $\Phi = 1.0$ , 1500 K, 1.3 atm. Filled squares and thin solid line, current study; cross-square, Niemitz et al. [4]; open triangle, Vermeer et al. [3]; open circle, Burcat et al. [2]; solid line (all data normalized to 1.3 atm by  $P^{-0.56}$ ), Davis and Law [9]; dashed line, Ranzi et al. [10]; dot-dashed line, Pitsch et al. [8]; dot-dot-dashed line, Curran et al. [7].

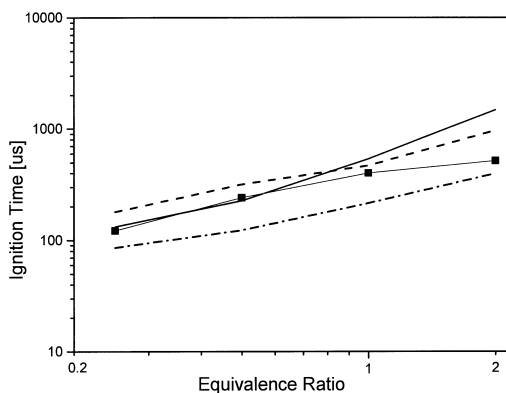


FIG. 5. Variation of ignition time with equivalence ratio for fixed O<sub>2</sub> concentration. Initial shock conditions: 6.25% O<sub>2</sub> 1500 K, 1.3 atm. Filled squares and thin solid line, current study; solid line, Davis and Law [9]; dashed line, Ranzi et al. [10]; dot-dashed line, Pitsch et al. [8].

there is strong evidence that the ignition times scale as  $P^{-0.56}$ , and this normalization is applied to all the data of Figs. 3–6.

The 1.3 atm, 0.5% data (shown in Fig. 3) have an activation energy of 43.9 kcal/mol, in relatively good overall agreement with all four models. All four models predict ignition times within a factor of two of the experiment. It should be noted that the current calculations were performed using a constant volume constraint and nitrogen as the carrier gas (as these mechanisms were optimized for air.) Small variations can exist between model predictions with

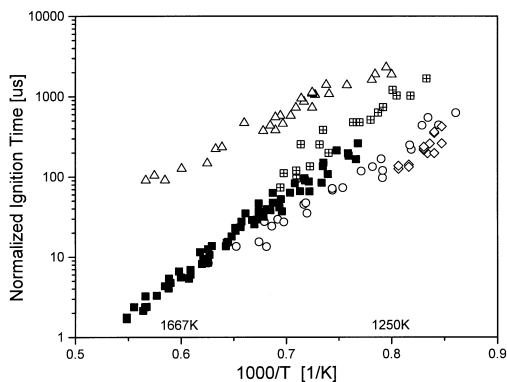


FIG. 6. Correlated ignition times: various shock tube studies. All data normalized to 1.3 atm and 1.68% iso-octane, 21% O<sub>2</sub> using  $P^{-0.56} \exp(-232X_{\text{fuel}})$ . Filled squares, current study; cross-squares, Niemitz et al. [4]; open triangles, Vermeer et al. [3]; open circles, Burcat et al. [2]; open diamonds, Nixon et al. [5].

M = Ar and M = N<sub>2</sub> because of the differences in heat capacity of Ar and N<sub>2</sub> (but this effect is likely to be small because of the low concentrations of reactants used in these experiments) and because of differences in the collision efficiencies of Ar and N<sub>2</sub> for dissociation reactions. However, the effects of these differences are minor on our calculations for  $T_{\text{ign}}$ . (See Ref. [18] for a study confirming this observation in CH<sub>4</sub> oxidation.)

The variation of ignition time with fuel concentration presented in Fig. 4 deviates from a simple power-law dependence. This is particularly evident at the highest concentrations where the present study shows a strong decrease in ignition time as concentration increases. This was also seen in the Burcat et al. [2] and the Niemitz et al. [4] data, but was not seen in the Vermeer et al. [3] data. At low to intermediate concentrations, the Ranzi et al. and the Davis and Law models closely follow the data, while the Pitsch et al. and Curran et al. models predict shorter ignition times by approximately a factor of two. At high concentrations, the four model predictions fall within the scatter of the three previous studies [2–4] and the current data.

The variation of the ignition time with equivalence ratio (presented in Fig. 5) shows a relatively weak effect on ignition time of fuel concentration for rich mixtures and fixed oxygen concentration. At 1500 K and 1.3 atm, as the equivalence ratio varies from 1.0 to 2.0, the measured ignition time only varies 29% from 400 to 515 μs. The Davis and Law, Pitsch et al., and Ranzi et al. mechanisms all predict similar variation of the ignition time with equivalence ratio for lean mixtures, but do not predict the rolloff for rich mixtures seen in the experiments.

The variation of ignition time with pressure and equivalence ratio can be scaled with some accuracy

assuming a simple power law [15]. However, the rapid decrease in ignition times with increased fuel concentration suggests that the variation of ignition time with fuel concentrations could be better correlated with an exponential function.

Using these relationships, a correlation for our 95 ignition time data points was found:

$$T_{\text{ign}} = 4.50 \times 10^{-10} P^{-0.56} \exp(-232X_{\text{fuel}}) \Phi^{1.62} \times \exp(44,780/R_{\text{[cal/mol/K]}} T) \quad (1)$$

with ignition time  $T_{\text{ign}}$  in seconds, pressure  $P$  in atmospheres, temperature  $T$  in degrees Kelvin fuel mole fraction  $X_{\text{fuel}}$ , and equivalence ratio  $\Phi$ . Data from the present work and from several other shock tube studies are normalized (for differences in  $P$  and  $X_{\text{fuel}}$ ) using this correlation and are presented in Fig. 6. Here, the data of Niemitz et al. are most consistent with the present study, and the ignition time data of Burcat et al. appear to converge with the current study at higher temperatures. The data of Vermeer et al. converges with the current data at lower temperatures, but diverge markedly at higher temperatures.

The highest quality shock tube data are obtained at very low fuel and oxidizer concentrations, and at short test times. With longer test times (>1 ms), shock tube data should be corrected for temperature and pressure changes resulting from increased boundary layer growth. With higher fuel concentrations, the temperatures and pressures that occur during the rapid release of energy during ignition are not well characterized. The current low-concentration data do not require significant correction, and should provide an accurate determination of ignition time over the conditions studied.

The accurate, low-scatter data in Figs. 3–5 and the correlation presented in equation 1 should be useful in testing the ability of current iso-octane mechanisms to predict changes in ignition time with pressure, fuel concentration, equivalence ratio, and temperature. For further evaluation of these detailed models, data on radical species concentration time histories are needed. These data is presented in the next section.

#### OH Laser Absorption Data

Representative OH concentration time histories (corrected) are shown in Fig. 7, and a comparison of one time history with modeling from several mechanisms is shown in Fig. 8.

Table 1 summarizes specific details of the OH concentration time-history profiles (corrected for interference absorption). In this table (and illustrated in Fig. 8),  $\tau_1(\text{peak})$ ,  $\tau_2(\text{min})$ , and  $\tau_3(50\%)$  are the times for the OH mole fraction to reach the first peak value, the minimum after this peak, and 50% of the second plateau level, respectively;  $X(1\text{st max})$ ,  $X(\text{min})$ , and  $X(2\text{nd max})$  are the OH mole fraction

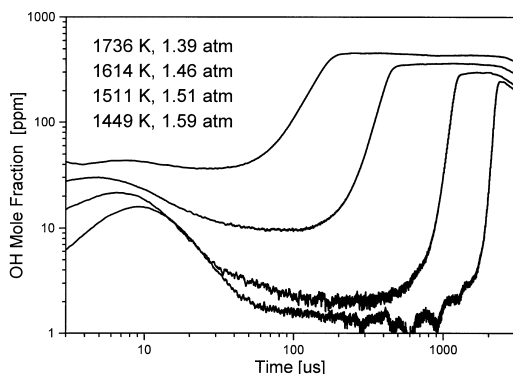


FIG. 7. OH absorption data (corrected). Initial conditions: 500 ppm, iso-octane, 0.625% O<sub>2</sub>. Upper trace, 1736 K; lower trace, 1449 K.

initial peak, the minimum or plateau value, and the postignition peak value, respectively.  $k_v$  is the absorption coefficient that was used to convert the measured absorbances to OH mole fraction [16].  $\tau_3(50\%)$  can be related to the ignition time. Model calculations indicate that  $\tau_3(50\%)$  is nearly coincident with the maximum of the CH concentration (which is closely equivalent to the maximum rate of change of the CH endwall emission) that occurs during the most rapid formation of radicals in the final

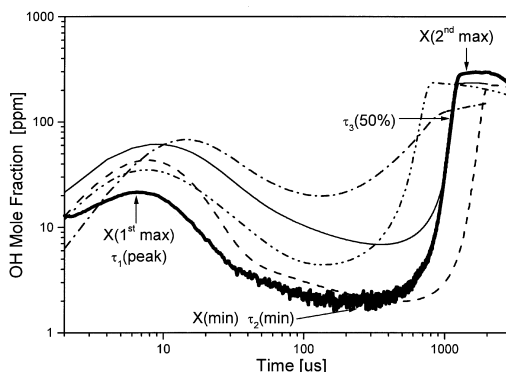


FIG. 8. OH absorption data (corrected) and comparison with models. Initial shock conditions: 500 ppm iso-octane, 0.625% O<sub>2</sub> 1511 K, 1.51 atm. Heavy solid line, measurement; solid line, Davis and Law [9]; dashed line, Ranzi et al. [10]; dot-dashed line, Pitsch et al. [8]; dot-dot-dashed line, Curran et al. [7].

stages of ignition. The measured values of  $\tau_3(50\%)$  are in good agreement with the simultaneously measured endwall ignition times if the small sidewall time correction of Petersen et al. [18] is applied. This correction is generally required for measurements of ignition time where the observation is made away from the endwall.

TABLE 1  
Summary of iso-octane OH absorption data

$T_5$ (K)	$P_5$ (atm)	$k_v$ (atm <sup>-1</sup> cm <sup>-1</sup> )	$\tau_1$ (peak)* ( $\mu$ s)	X (1st max) (ppm)	$\tau_2$ (min)* ( $\mu$ s)	X (min) (ppm)	$\tau_3$ (50%)* ( $\mu$ s)	X (2nd max) (ppm)
0.05% iso-octane, 0.625% O <sub>2</sub>								
1736	1.399	132	5	44	27	36	137	456
1614	1.463	151	5	30	86	9	388	352
1511	1.511	173	6	22		2	1152	288
1449	1.593	185	8	16		1	2182	245
0.25% iso-octane, 6.25% O <sub>2</sub>								
1570	1.412	160		159		42	62	Sat. <sup>a</sup>
1467	1.482	178	3	93	14	12	226	Sat.
1394	1.533	198	4	49	49	2	621	Sat.
1299	1.625	209	6	16		1	1825	Sat.
0.5% iso-octane, 6.25% O <sub>2</sub>								
1507	1.435	154		100		7	280	Sat.
1641	1.373	148		149	12	34	62	Sat.
1408	1.495	190	3	42		2	880	Sat.
1330	1.554	205	4	17		4	1870	Sat.
1.0% iso-octane, 6.25% O <sub>2</sub>								
1322	1.576	206	3	12		1		Sat.
1398	1.491	192		31		1	1422	Sat.
1506	1.418	172		26		3	589	Sat.
1656	1.336	147		103	17	12	127	Sat.

<sup>a</sup>Sat. = transmission  $\sim 0$ .



As can be seen in Fig. 7, all OH absorption data show evidence of the same concentration time history structure. At early times, there is a rapid formation of OH to a peak  $X(1st\ max)$  simultaneous with the initial decomposition of the fuel molecule. The OH concentration then falls to a well-defined plateau  $X(min)$ , during the induction period. The scavenging effect of iso-octane and its decomposition products on the radical population is clearly evident in the suppressed levels of OH that occur in this plateau  $X(min)$ . This suppression is especially evident when compared to similar measurements done in *n*-heptane [12] where the OH plateau level before ignition does not drop below its initial formation peak. In the rapid final ignition process, OH concentration rises to the postignition plateau  $X(2nd\ max)$  and then rounds smoothly to a second plateau. This second plateau level falls slowly over the recorded millisecond times scale of these experiments as slower three-body recombination processes take place.

The predictions of the four mechanisms are compared with one example OH concentration time history data trace in Fig. 8. All four mechanisms capture the general form of the OH concentration profile. The Ranzi et al. mechanism most closely models the strong suppression of the OH radicals before ignition, but both the Ranzi et al. and the Curran et al. mechanisms do a reasonable job at modeling the full profile, predicting within a factor of two, the initial OH peak. The smaller Davis and Law and Pitsch et al. mechanisms overpredict the minimum OH by factors of 3 and 10, respectively, and the first peak by a factor of 3, though the Davis and Law mechanism still does an excellent job at predicting the ignition times.

Sensitivity analysis using the Davis and Law mechanism for the conditions of Fig. 8 indicate that at early times the formation of the first OH peak is controlled by the reactions:  $H + O_2 \rightarrow O + OH$ , iso-octane  $\rightarrow t-C_4H_9 + i-C_4H_9$ , iso-octane  $\rightarrow C_7H_{15} + CH_3$ , and  $i-C_3H_7 \rightarrow H + C_3H_6$ ; the subsequent OH removal is controlled by:  $i-C_3H_7 \rightarrow CH_3 + C_2H_4$ . As expected for this branched alkane, the fate of OH radicals is intimately related to the choice of decomposition pathways and rates for iso-octane, and improvements to the modeling of this early time OH are likely possible by adjusting the rates of these pathways within their uncertainty limits.

During the OH plateau minimum, contribution analysis indicates that there is a competition between OH formation by  $H + O_2$  and OH removal by reaction with  $H_2$ ,  $CH_3$ ,  $CH_2O$ ,  $C_2H_6$ , and other intermediate product species. The OH formation rate is sensitive to the fate of H-atoms and therefore shows a strong sensitivity to reactions such as  $H + C_3H_5$ , and  $H + C_3H_6$  that remove H-atoms, and  $HCO + O_2$  that lead to formation of H-atoms. Improvements in modeling the plateau minimum may

come from the inclusion of a fuller complement of H-abstraction reactions for the intermediate olefins and OH removal reactions for all intermediate species, as well as adjustment of critical rate coefficients.

While ignition time and OH data help identify key reactions, the next steps in mechanism improvement are: (1) adjustment of critical rate coefficients, within their uncertainties; (2) direct studies of key reaction rates where they are uncertain; (3) measured time histories of other species, for example,  $CH_3$ , to further constrain the models; and (4) comparative investigations of other branched alkanes, for example, iso-butane and iso-pentane, which would provide information on related kinetic structure.

## Conclusions

A new database of ignition times and OH radical concentration time histories was generated for iso-octane ignition. A comparison of the ignition time data with a variety of current iso-octane oxidation mechanisms revealed that these mechanisms replicate some of the features of the ignition time data reasonably well, but do not accurately capture the temperature dependence of the ignition time or the rolloff behavior with rich equivalence ratios. As well, caution is advised when selecting modeling targets ignition times at high concentrations, because not all the published data are consistent with the present study. A comparison of the measured OH time histories with several recent models reveals that wide variations occur in the predictions of the OH concentration time histories especially for the smallest reduced mechanisms. Researchers engaged in model development should find these new data helpful in refining their models and when used in conjunction with similar data for *n*-heptane performed in our laboratory [12] should provide a new database for primary reference fuel mechanism validation.

## Acknowledgments

This work was supported by the Army Research Office with Dr. David Mann as contract monitor. We were assisted with the OH absorption measurements by C. Libby who is supported by an NSF fellowship.

## REFERENCES

1. Roberts, C. E., Matthews, R. D., and Leppard, W. R., SAE technical paper 96-2107.
2. Burcat, A., Pitz, W. J., and Westbrook, C. K., *Proc. Intl. Conf. Shock Waves* 18:771-780 (1991).
3. Vermeer, D. J., Meyer, J. W., and Oppenheim, A. K., *Combust. Flame* 18:327-336 (1972).
4. Niemitz, K. J., Zellner, R., Esser, C., and Warnatz, J., data reproduced in C. K. Westbrook, J. Warnatz, and W. J. Pitz, *Proc. Combust. Inst.* 22:893-901 (1988).

5. Nixon, A. C., Ackerman, G. H., Hawthorn, R. D., Henderson, H. T., and Ritchie, A. W., technical documentary report APL-TDR-64-100 Part III, Air Force Aero Propulsion Laboratory, Wright-Paterson AFB, 1966.
6. Fiewieger, K., Blumenthal, R., and Adomeit, G., *Combust. Flame* 109:599–619 (1997).
7. Curran, H. J., Pitz, W. J., Westbrook, C. K., Callahan, C. V., and Dryer, F. L., *Proc. Combust. Inst.* 27:379–387 (1998).
8. Pitsch, H., Peters, N., and Seshadri, K., *Proc. Combust. Inst.* 26:763–771 (1996); Pitsch, H., personal communication, 2001.
9. Davis, S. G., and Law, C. K., *Proc. Combust. Inst.* 27:521–527 (1998).
10. Ranzi, E., Faravelli, T., Gaffuri, P., Sogaro, A., D'Anna, A., and Ciajolo, A., *Combust. Flame* 108:24–42 (1997).
11. Held, T. J., Marchese, A. J., and Dryer, F. L., *Combust. Sci. Technol.* 123:107–146 (1997).
12. Davidson, D. F., Herbon, J. T., Horning, D. C., and Hanson, R. K., *Int. J. Chem. Kinet.* 33:775–783 (2001).
13. Horning, D. C., Davidson, D. F., and Hanson, R. K., “Shock Tube Study of the High-Temperature Thermal Decomposition of *n*-Alkanes,” paper 5731, Twenty-Third Symposium on Shock Waves; Horning, D. C., *Study of the High-Temperature Auto-ignition and Thermal Decomposition of Hydrocarbons*, Stanford University Mechanical Engineering Department report TSD-135, Stanford University, CA, June 2001.
14. Burcat, A., and McBride, B., *Ideal Gas Thermodynamic Data for Combustion and Air-Pollution Use*, Technion Aerospace Engineering (TAE) report 804, Technion University, Israel, June 1997.
15. Horning, D. C., Davidson, D. F., and Hanson, R. K., *J. Propul. Power* 18:363–371 (2002).
16. Herbon, J. T., Hanson, R. K., Golden, D. M., and Bowman, C. T., *Proc. Combust. Inst.* 29:1201 (2002).
17. Davidson, D. F., Horning, D. C., Herbon, J. T., and Hanson, R. K., *Proc. Combust. Inst.* 28:1687–1692 (2000).
18. Petersen, E. L., Davidson, D. F., and Hanson, R. K., *J. Propul. Power* 15:82–91 (1999).

## COMMENTS

*Frederick L. Dryer, Princeton University, USA.* In the comparison with your shock tube ignition delay data with those of other investigators, did you consider that temperature corrections of the calculated temperature might be of different magnitudes in the different experiments?

Do you have any mechanistic or experimental explanation for the observation of the initial OH “spike” found in experiments and not shown by any of the mechanisms?

*Author's Reply.* We did not attempt to apply any temperature corrections to our data or to the published data of other groups when we compared them. If shock tubes of substantially smaller diameters are used for ignition time measurements, there may, however, be some reduction in the apparent activation energy due to boundary-layer-induced temperature increases that occur in shock tubes at longer test times.

For a very short duration ( $\sim 3 \mu\text{s}$ ) during the passage of the shock front across the laser beam path, the shock front

momentarily steers the diagnostic beam away from the detector surface. This generates a sharp oscillation in the absorption data at time zero. This spike has no chemical kinetic significance.

•

*William J. Pitz, Lawrence Livermore Laboratory, USA.* In our work on the autoignition of iso-octane/air mixtures under conditions related to argone knock, we also found that the OH concentration was suppressed prior to hot ignition. We determined through chemical kinetic modeling that the formation of iso-butane from iso-octane and the reaction of iso-butene with OH removes OH from the system. This reaction leads to resonantly stabilized iso-butenyl radicals and chain termination.

*Author's Reply.* Thank you for your comment.